ETH
Eidgenössische Technische Hochschule Zürich
Swiss Federal Institute of Technology Zurich

Seminar for Applied Mathematics SAM

Harmonic Balance Techniques in Cardiovascular Fluid Mechanics

T. S. Koltukluoglu

Research Report No. 2019-55
September 2019

Seminar für Angewandte Mathematik
Eidgenössische Technische Hochschule
CH-8092 Zürich
Switzerland

Harmonic Balance Techniques in Cardiovascular Fluid Mechanics

Taha Sabri Koltukluoğlu[1], Gregor Cvijetić[2], and Ralf Hiptmair[1]

[1] Seminar for Applied Mathematics, ETH, Zurich, CH
ktaha@ethz.ch
[2] Faculty of Mechanical Engineering and Naval Architecture, FSB, Zagreb, HR

Abstract. In cardiovascular fluid mechanics, the typical flow regime is unsteady and periodic in nature as dictated by cardiac dynamics. Most studies featuring computational simulations have approached the problem exploiting the traditional mathematical formulation in the time domain, an approach that incurs huge computational cost. This work explores the application of the harmonic balance method as an alternative numerical modeling tool to resolve the dynamic nature of blood flow. The method takes advantage of the pulsatile regime to transform the original problem into a family of equations in frequency space, while the combination of the corresponding solutions yields the periodic solution of the original problem. As a result of this study we conclude that only a few harmonics are required for resolving the presented fluid flow problem accurately and the method is worth of further investigation in this field.

1 Introduction

In cardiac dynamics, blood flow is heavily influenced by the dynamic nature of the heart beat, which results in an unsteady and periodic flow. When performing pulsatile flow simulations, the classical approach relies on the traditional time-stepping schemes, which require the definition of boundary conditions (BCs) at every time instant. In recent decades, phase-contrast magnetic resonance imaging (4D flow MRI) became relevant for data-based computational fluid dynamics (CFD) studies. Velocity components of blood flow can be measured in-vivo and non-invasively. In addition, three-directional flow can be resolved with the ability to measure the temporal evolution of blood flow within a 3D volume [7]. In CFD studies relying on 4D flow MRI data, sparsely measured velocity profiles are usually interpolated to generate velocity fields to be applied as dynamic BCs for each time instant. Such studies simply apply either linear or spline interpolation [11, 8] for transient CFD simulations. Most of these studies have approached the transient problem exploiting the traditional mathematical formulation in the time domain, an approach that incurs huge computational cost.

In this work, an alternative and effective approach is proposed for temporal discretization. This method is known as the harmonic balance (HB) approach [6], so far mostly reported with preliminary results using mostly 2D or idealized cylindrical geometries [10, 4, 3]. To the best of authors' knowledge, the HB

method is investigated in this work for the first time in the field of computational hemodynamics. The method is based on Fourier decomposition of the velocity field in time and enables the evaluation of its derivative with respect to time in frequency space. Furthermore, the HB discretization can easily be adapted to the sampling rate of measurements in time. This eliminates the necessity for completing the missing data for all time steps, as required in conventional methods. In 4D flow MRI, the velocity components are usually obtained by periodic averaging. The proposed method makes use of this information and proves to be accurate and remarkably effective in terms of computational time.

2 Mathematical Model

Let $\Omega \subset \mathbb{R}^3$ be an open set with boundary $\partial\Omega = \Gamma_i \cup \Gamma_o \cup \Gamma_w$. See Figure 1a, where Γ_i, Γ_o and Γ_w represent the inlet, outlet and wall boundaries respectively. An incompressible Newtonian fluid is assumed to flow through Ω in the time interval $\mathbb{T} := [0; T]$, as the result of prescribed T-periodic inflow data at Γ_i. The velocity field prescribed at the inlet is characterized by the T-periodic function $g(t, x) = g(t + mT, x) : \mathbb{T} \times \Gamma_i \to \mathbb{R}^3$ with $m \in \mathbb{N}$. The density and dynamic viscosity of the fluid are denoted as ρ and μ respectively.

Considering the strain rate tensor $\nabla^s(\cdot) = [\nabla(\cdot) + (\nabla(\cdot))^T]/2$ and setting $\mathcal{U} = \left\{ v \in H^1(\Omega) \mid v|_{\Gamma_w} = \mathbf{0} \right\}$, the Navier-Stokes equations read: for $t \in \mathbb{T}$, given the initial guess $u(0, x) = u(x)^{\{0\}}$, find $(u, p) \in \mathcal{U} \times L^2(\Omega)$, such that

$$\rho\,[\,\partial_t u + (\nabla u)u\,] - \mu\Delta u + \nabla p = \mathbf{0} \qquad \text{in } \mathbb{T} \times \Omega \ , \tag{1}$$

$$\operatorname{div} u = 0 \qquad \text{in } \mathbb{T} \times \Omega \ , \tag{2}$$

$$u = g \qquad \text{on } \mathbb{T} \times \Gamma_i \ , \tag{3}$$

$$(-pI + 2\mu\nabla^s u)n = \mathbf{0} \qquad \text{on } \mathbb{T} \times \Gamma_o \ . \tag{4}$$

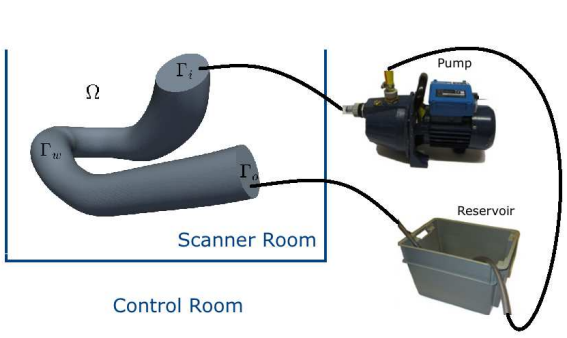

(a) Flow Domain and Experimental Setup

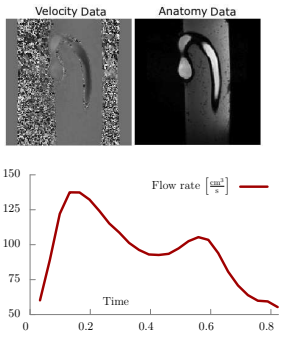

(b) Flow Rate

Fig. 1. Experimental setup (a) and flow rate waveform (b) obtained from 4D flow MRI acquisition in flow domain Ω with boundaries Γ_i : inlet, Γ_o : outlet and Γ_w : wall.

2.1 Harmonic Balance

In what follows, we will consider a time discretization of the momentum equation (1), which can be expressed in the following compact form

$$\partial_t u = f(u), \tag{5}$$

where $f(u) := -\Big[(\nabla u)u - \nu\Delta u + \frac{\nabla p}{\rho}\Big]$ (with $\nu := \frac{\mu}{\rho}$ being the kinematic viscosity), which encompasses the convective and diffusive terms along with the force term caused by the pressure. Equation (5) is an evolution equation. Further, $t \to u(t,x)$ is periodic in time with known period T. Therefore, we approximate $u \approx \tilde{u}(t,x) = \sum_{k=1}^{2n+1} c_k(x)\varphi_k(t)$ with the temporal expansion functions φ_k taken from the set

$$\mathcal{T} := \{\, 1, \cos(\omega t), \sin(\omega t), \cos(2\omega t), \sin(2\omega t), \cdots, \cos(n\omega t), \sin(n\omega t)\,\}, \tag{6}$$

where $\mathcal{T}$ represents a complete L^2-orthogonal system on $\mathbb{T}$ and $\omega = \frac{2\pi}{T}$ is the angular frequency. This gives rise to a Fourier spectral method [1] for approximation in time, which relies on the degree-n Fourier polynomial

$$\tilde{u}(t,x) = \frac{\hat{u}_{c_0}(x)}{2} + \sum_{k=1}^{n}\Big[\hat{u}_{c_k}(x)\cos(k\omega t) + \hat{u}_{s_k}(x)\sin(k\omega t)\Big], \tag{7}$$

where $\hat{u}_{c_k}$ for $k = 0\cdots n$ and $\hat{u}_{s_k}$ for $k = 1\cdots n$ form the discrete spectrum of $\tilde{u}$.

In order to obtain a system of equations for the discrete spectrum, we demand that equation (5) be satisfied for $2n+1$ time instants denoted as t_j. We employ a collocation approach and opt for equidistant collocation points

$$t_j := \frac{jT}{2n+1}, \quad j = 1, 2, \cdots, 2n+1. \tag{8}$$

The number of collocation points is equal to the number of terms in the Fourier polynomial (7). Finally, inserting (7) into (5), applying the derivative and demanding that (5) be satisfied at each t_j, the following $2n+1$ equations are obtained in the frequency domain

$$\sum_{k=1}^{n}\Big[\hat{u}_{s_k} k\omega\cos(k\omega t_j) - \hat{u}_{c_k} k\omega\sin(k\omega t_j)\Big] = f(t_j, \tilde{u}(t_j,x)), \quad j = 1\cdots 2n+1. \tag{9}$$

Let $\tilde{u}^{\,i} := \tilde{u}(t_i, x)$ be the approximated velocity field at time instant t_i. The DFT of $\tilde{u}^i$ is given by the discrete cosine and sine transforms $\hat{u}_{c_k} = \frac{2}{2n+1}\sum_{i=1}^{2n+1}\tilde{u}^{\,i}\cos(k\omega t_i)$ and $\hat{u}_{s_k} = \frac{2}{2n+1}\sum_{i=1}^{2n+1}\tilde{u}^{\,i}\sin(k\omega t_i)$. Inserting the discrete spectrum into the equations in (9) and using the trigonometric identities, $\sin(\alpha\pm\beta) = \sin(\alpha)\cos(\beta)\pm\cos(\alpha)\sin(\beta)$, results in the following approximation,

$$\begin{aligned}\sum_{k=1}^{n}\Big[\,\frac{2k\omega}{2n+1}\sum_{i=1}^{2n+1}\tilde{u}^{\,i}\Big(\sin(k\omega t_i)\cos(k\omega t_j) - \cos(k\omega t_i)\sin(k\omega t_j)\Big)\,\Big] &= f(t,\tilde{u})\\ \Rightarrow\ \frac{2\omega}{2n+1}\sum_{i=1}^{2n+1}\sum_{k=1}^{n} k\tilde{u}^{\,i}\sin(k\omega(t_i - t_j)) &= f(t,\tilde{u})\,.\end{aligned} \tag{10}$$

Setting $N = 2n+1$ and defining $c_{ij} = \frac{2\omega}{N} \sum_{k=1}^{n} k \sin(k\omega(t_i - t_j))$ for $i, j = 1 \cdots N$, we finally obtain from (10) the harmonically balanced momentum equations

$$\sum_{i=1}^{N} \tilde{u}^{\,i} c_{ij} + (\nabla \tilde{u}^{\,j}) \tilde{u}^{\,j} - \nu \Delta \tilde{u}^{\,j} + \frac{\nabla p^j}{\rho} = \mathbf{0}\,, \qquad j = 1, 2, \cdots, N. \tag{11}$$

The frequency domain equations are now expressed in terms of the time domain state variables $\tilde{u}^{\,j}$ at each time instant $t_j = \frac{jT}{2n+1}$. The original problem has been cast into the form of a set of coupled fluid flow problems, which yield the periodic solution of the original problem.

For the set of HB momentum equations (11), the SIMPLE algorithm [9] was employed to deal with the pressure-velocity coupling at each time instant t_j, separately. The temporal influence from neighbouring time instants is accounted for by the summation term $\sum_{i=1}^{N} \tilde{u}^{\,i} c_{ij}$. The numerical solution of the HB coupling is obtained using a block-Gauss-Seidel iterative algorithm. The spatial discretization of the corresponding equations was achieved using the finite volume method. Algorithm 1 describes the HB method in terms of a pseudo-code. The fields $(\cdot)^{\{k\}}$ will represent the fields $(\cdot)$ at k-th iteration of SIMPLE. Moreover, the equation residuals of the equations in (11) will be denoted by $\mathscr{R}^j((u^j)^*)$ for each j, where $(u^j)^*$ is the corresponding approximation of the solver. The calculation is considered converged when each of the N equation sets are converged.

Algorithm 1 SIMPLE & Block-Gauss-Seidel Algorithm for Harmonic Balance

Input : $(u^j)^{\{0\}}$, $(p^j)^{\{0\}}$, n ▷ Initial guesses $(\cdot)^{\{0\}}$ and harmonics

Output : $(u^j)^{\{k\}}, (p^j)^{\{k\}}$ ▷ Flow fields at last iteration k

procedure HarmonicBalanceLoop($u^{\{0\}}, p^{\{0\}}, N = 2n+1$)

  $g^j \leftarrow (u^j)^{\{0\}}$ on Γ_i for $j = 1 \cdots N$, $m \leftarrow$ Number of HB iterations

  for $k \leftarrow 1, m$ **do** ▷ HB iterations

    for $j \leftarrow 1, N$ **do** ▷ Solve one SIMPLE iteration at each t_j

      $(u^j)^{\{k\}} \leftarrow$ Given $\sum_{i=1}^{N} \tilde{u}^{\,i} c_{ij}$, g^j, $(p^j)^{\{k-1\}}$ solve equation (11)

      $(p^j)^{\{k\}} \leftarrow$ Given $(u^j)^{\{k\}}$ solve for $(p^j)^{\{k\}}$

      Correct $(u^j)^{\{k\}}$ using $(p^j)^{\{k\}}$ and update HB coupling $\sum_{i=1}^{N} \tilde{u}^{\,i} c_{ij}$

    if each $|\mathscr{R}^j((u^j)^{\{k\}})| \ll 1$ **then** ▷ Convergence criterion

      return $(u^j)^{\{m\}}, (p^j)^{\{m\}}$ for $j = 1 \cdots N$

3 Experimental Setup for 4D flow MRI

A time-dependent experiment was performed using a glass replica of human aorta, which was placed in a 3T MRI scanner. The rigid geometry consists of aortic root, ascending aorta, aortic arch without branches and descending aorta as illustrated in Figure 1a. Detailed explanation of the experimental setup is provided in [5] (Section 5.1). The acquired voxel size was 1.5 mm^3 isotropic, along with a time resolution of 33 ms. The period of one heart cycle was 0.825 seconds and 25 data were acquired per cardiac cycle. Controlling the flow rates, a Reynolds number of at most 1100 was achieved. The flow model in this work does not account for turbulence, which is a matter of current research. Finally, the obtained volumetric flow rate resulted in a wave containing two peaks of different magnitudes as shown in Figure 1b. The observed flow rates are merely an approximation to the physiological flow rates and were dictated by limitations of the experimental setup.

The connection was made with a PVC tubing of total length 20 m with an inner diameter of 19 mm. The inlet and outlet of the pipe were connected to a reservoir in the control room creating an open circuit. A ball bearing valve was placed 1.5 m downstream the tube and was used to control the flow rate. Figure 1a illustrates the experimental setup.

Obtained raw measurements underwent a set of preprocessing tasks including denoising of the flow field, segmentation of the aorta, its smoothing and registration with the exact geometry and a divergence-free projection of the reconstructed flow field, which have all been comprehensively described in [5] (Sections 3 and 5.3). Further, three computational meshes, denoted as $\mathbf{M_2}$, $\mathbf{M_4}$ and $\mathbf{M_7}$, were generated using the exact geometry of the aortic replica, with different numbers of cells, 215 000, 440 000 and 750 000 respectively.

In addition to the flow acquisition, reference flow solutions were numerically generated to serve as the ground truth for validation purposes. To achieve this, first an inflow boundary profile was reconstructed from a single steady-state flow MRI acquisition and the obtained flow field was smoothed using low-pass filtering (in order to reduce the measurement noise). Second, the acquired steady flow profile was dynamically adjusted over time and then applied as BC at the inlet for twenty periods to achieve a transient flow simulation with a periodic state of equilibrium. This was performed by multiplying each velocity component at the inlet with an appropriately chosen analytical periodic function of period 0.8 s and base frequency of 1.25 Hz. The function was chosen such that it contains two peaks of different magnitudes in one cycle, similar to the flow rates obtained from the dynamic experiments.

4 Numerical Experiments

Computed flow fields u_c and reference flow fields u_r were quantitatively compared using the following normalized root-mean square error integrated over time

$$\mathrm{nRMSE}(u_c, u_r) = \left(\frac{100}{\underset{\mathbb{T},\Omega}{\mathrm{avr}}|u_r|} \right) \sqrt{\frac{1}{V_\Omega \cdot T} \int_{\mathbb{T}} \int_{\Omega} |u_c - u_r|^2 \, d\Omega \, dt}. \tag{12}$$

Validation with a Single Mesh Geometry As a first step, mesh $\mathbf{M_2}$ was employed to generate both the numerical reference solution, denoted by $u_{\mathbf{ext}}$, as well as the solutions based on the HB method, denoted by $u^n_{\mathbf{hb}}$ with $n = \{2, 5, 8, 10, 12\}$ number of harmonics. For this purpose, the reference flow solution was sparsely sampled multiple times at $2n+1$ equidistantly placed time instants for each HB simulation, resulting in 5, 11, 17, 21 and 25 data points (samples) per cycle respectively. The samples were then used as the observational boundary data for the HB solver, which was run for 1 000 Gauss-Seidel iterations on mesh $\mathbf{M_2}$ using 48 processors. Quantitatively, the solutions $u^n_{\mathbf{hb}}$ were compared with the reference solution $u_{\mathbf{ext}}$ in terms of nRMSE($u^n_{\mathbf{hb}}$, $u_{\mathbf{ext}}$), resulting in 13.22%, 2.18%, 0.75%, 0.43% and 0.29% respectively. These results are summarized in Table 1 along with the corresponding wall clock times.

Table 1. Root mean square errors nRMSE($u^n_{\mathbf{hb}}, u_{\mathbf{ext}}$) evaluated against the ground truth $u_{\mathbf{ext}}$ and the corresponding wall clock times (WCT) in seconds.

u_c	$u^2_{\mathbf{hb}}$	$u^5_{\mathbf{hb}}$	$u^8_{\mathbf{hb}}$	$u^{10}_{\mathbf{hb}}$	$u^{12}_{\mathbf{hb}}$
nRMSE(u_c, $u_{\mathbf{ext}}$)	13.22%	2.18%	0.75%	0.43%	0.29%
WCT in seconds	217 s	458 s	788 s	960 s	1 190 s

We observed that at least 8 harmonics are needed for the HB method to recover the velocity field with nRMSE below 1%. Considering the number of harmonics from 2 to 12, the errors dropped rapidly (from 13.22% to 0.29%), whereas further increase in the number of harmonics over 12 did not drastically improve the flow field. Finally, we conclude that the use of a moderate number of harmonics, e.g. between 8 and 12, is enough to reconstruct the flow field with an acceptable accuracy (errors below 1%). Hereafter, we make use of the HB method set with 12 harmonics. The corresponding HB solution is simply referred to as $u_{\mathbf{hb}}$ (instead of $u^{12}_{\mathbf{hb}}$).

Sensitivity to the Mesh Size Parameter To further verify the processes, a much finer mesh, denoted by $\mathbf{M_7}$, was used to generate the numerical reference solution, denoted by $u_{\mathbf{ext}}$ and sampled at 25 time instants. The reference solution

was then mapped to the meshes $\mathbf{M_2}$ and $\mathbf{M_4}$ using a cell volume weighted interpolation method [2] and resulting in reference flow fields denoted by $u^2_{\mathbf{ext}}$ and $u^4_{\mathbf{ext}}$ respectively. As such, there is now a source of error in terms of interpolation. In mesh $\mathbf{M_2}$, nRMSE($u_{\mathbf{hb}}$, $u^2_{\mathbf{ext}}$) was 2.93%, whereas, in mesh $\mathbf{M_4}$, the same metric evaluated against $u^4_{\mathbf{ext}}$ was 1.51%.

4.1 Comparison with a Classical Data-based CFD Method

As additional validation of the HB method, we have considered a classical CFD approach based on traditional time-stepping schemes for comparison purposes. Instead of using a simple linear interpolation, we consider an inverse problem based on penalized regression spline (PRS) to reconstruct the inflow BCs at all time instants present in the traditional time discretization, for which the observations are not available. The regression model functions are of class C^2 and correspond to cubic splines with uniformly distributed nodes. For the PRS method, the momentum equation was discretized in time using backward differentiation, an implicit scheme of second order accuracy. The time steps were chosen such that the Courant number was below 0.3.

The simulations with the HB and PRS methods were run in computational meshes $\mathbf{M_2}$ and $\mathbf{M_4}$, using 48 and 96 processors respectively. The PRS simulation was run for 12 periods, where a periodic state of equilibrium was reached. The velocity fields $u_{\mathbf{hb}}$ and $u_{\mathbf{prs}}$, numerically obtained from HB and PRS methods respectively, were compared with the exact solution. The results are summarized in Table 2. Remarkably, the HB method yields almost the same accuracy as the

Table 2. Root mean square errors (nRMSE($u_{\mathbf{hb}}, u^n_{\mathbf{ext}}$) and nRMSE($u_{\mathbf{prs}}, u^n_{\mathbf{ext}}$) for HB and PRS methods, evaluated against the reference solutions $u^2_{\mathbf{ext}}$ and $u^4_{\mathbf{ext}}$ mapped onto meshes $\mathbf{M_2}$ and $\mathbf{M_4}$ respectively. In addition, the corresponding wall clock times (WCT) in seconds is provided for each simulation (with 96 processors) on $\mathbf{M_4}$.

u_c	nRMSE(u_c, $u^2_{\mathbf{ext}}$) on $\mathbf{M_2}$	nRMSE(u_c, $u^4_{\mathbf{ext}}$) on $\mathbf{M_4}$	WCT for u_c on $\mathbf{M_4}$
$u_{\mathbf{hb}}$	2.93%	1.51%	1 512 s
$u_{\mathbf{prs}}$	2.88%	1.47%	23 052 s

PRS method, when compared with a reference solution. Furthermore, the error nRMSE($u_{\mathbf{hb}}$, $u_{\mathbf{prs}}$) between these solutions was 0.39% in $\mathbf{M_2}$ and 0.36% in $\mathbf{M_4}$. Finally, the WCT in $\mathbf{M_4}$ were 23 052 s for the PRS method and 1 512 s for the HB method, the latter being ≈ 15 times faster than the former. In total, the PRS method needed ≈ 6.4 hours, whereas the HB method with $n = 12$ needed ≈ 25 minutes. This is a tremendous saving in terms of computational effort.

4.2 Simulations with Boundary Data from 4-D Flow MRI

The performance and feasibility of both the HB and PRS methods was studied on $\mathbf{M_2}$ to reconstruct the velocity fields obtained from 4D flow MRI experiment. Computed flow patterns were first qualitatively compared by visual inspection. The HB method proved to be able to reproduce the velocity field delivered by the PRS method without an appreciable difference. Finally, since no ground truth is available, the velocity fields obtained from HB and PRS methods were quantitatively compared, resulting in a metric nRMSE($u_{\mathbf{hb}}$,$u_{\mathbf{prs}}$) of 8.56%.

5 Conclusions

This work has investigated the harmonic balance method as a novel approach to perform pulsatile fluid flow simulations in computational hemodynamics, facilitating the combination of CFD with data obtained from 4D flow MRI. The method is being reported for the first time in a study combining CFD with 4D flow MRI and it shows a significant improvement regarding the trade-off between computational cost and accuracy.

Comparison has been performed against a classical CFD method based on a traditional time discretization scheme. The classical approach proves to be a time consuming process. In contrast, the harmonic balance method relies on a frequency-based temporal discretization scheme. Thereby, the velocity field is decomposed into its Fourier series and the method operates in the frequency domain. Based on our experiments, the harmonic balance method was about 15 times faster compared to the conventional transient simulations.

Our experience indicates that only a moderate number of harmonics is required to accurately resolve the periodic fluid flow problem. This makes the method extremely useful, for example, in data assimilation procedures based on 4D flow MRI acquisitions, where the fluid flow problem has to be solved many times. Regarding the number of time instants at which data is acquired per cardiac cycle, the method can be easily adjusted such that the discretized momentum equations are temporally registered with the measurements. In the case of 4D flow MRI, our experience indicates that it requires observational data at a number of time instants between 17 and 25. This corresponds to a number of harmonics of at least 8, which is a region in which the method has proved to be satisfactorily accurate.

This work does not include the mechanical models of the vessel walls but is a starting point for the adaptation of fluid-structure interaction studies. Hence, this investigation is the first of a series that will most likely address the deformation and dynamic response of the arterial walls.

Based on these results, we conclude that the HB numerical scheme reveals itself as a method with a tremendous potential in computational hemodynamics. The proposed approach enables pulsatile fluid flow simulations at a significantly smaller cost when compared with traditional methods, without exhibiting deterioration of the approximate solution.

References

1. Boyd, J.: Chebyshev and Fourier Spectral Methods: Second Revised Edition. Dover Books on Mathematics, Dover Publications (2001)
2. Coetzee, R.V.: Volume weighted interpolation for unstructured meshes in the finite volume method. Ph.D. thesis, North-West University (2005)
3. Cvijetić, G., Jasak, H., Vukčević, V.: Finite volume implementation of the harmonic balance method for periodic non-linear flows. 4th AIAA Aerospace Sciences Meeting (2016). https://doi.org/10.2514/6.2016-0070
4. Hall, K.C., Ekici, K., Jeffrey, P.T., Earl, H.D.: Harmonic balance methods applied to computational fluid dynamics problems. Int. J. Comput. Fluid Dynam. **27**(2), 52–67 (2013). https://doi.org/10.1080/10618562.2012.742512
5. Koltukluoğlu, T.S., Blanco, P.J.: Boundary control in computational haemodynamics. J. Fluid Mech. **847**, 329–364 (2018). https://doi.org/10.1017/jfm.2018.329
6. Krack, M., Gross, J.: Harmonic Balance for Nonlinear Vibration Problems. Springer, Cham (2019). https://doi.org/10.1007/978-3-030-14023-6
7. Markl, M., Frydrychowicz, A., Kozerke, S., Hope, M., Wieben, O.: 4D flow MRI. Magn. Reson. Im. **36**(5), 1015–1036 (2012). https://doi.org/10.1002/jmri.23556
8. Miyazaki, S., Itatani, K., Furusawa, T., Nishino, T., Sugiyama, M., Takehara, Y., Yasukochi, S.: Validation of numerical simulation methods in aortic arch using 4d flow mri. Heart and Vessels **32**(8), 1032–1044 (2017). https://doi.org/10.1007/s00380-017-0979-2
9. Patankar, S.V., Spalding, D.B.: A calculation procedure for heat, mass and momentum transfer in three-dimensional parabolic flows. J. Heat Mass Transfer **15**, 1787–1806 (1972). https://doi.org/10.1016/0017-9310(72)90054-3
10. Stokes, A.: On the approximation of nonlinear oscillations. J. Differ. Equ. **12**(3), 535–558 (1972). https://doi.org/10.1016/0022-0396(72)90024-1
11. Wake, A.K., Oshinski, J.N., Tannenbaum, A.R., Giddens, D.P.: Choice of in vivo versus idealized velocity boundary conditions influences physiologically relevant flow patterns in a subject-specific simulation of flow in the human carotid bifurcation. J. Biomech. Eng. **131**(2) (2009). https://doi.org/10.1115/1.3005157